T1-B

PHYSICAL REVIEW C **72**, 064317 (2005)

Relativistic transport approach to collective nuclear dynamics

Serbülent Yildirim,[1] Theodoros Gaitanos,[2] Massimo Di Toro,[3,*] and Vincenzo Greco[3]
[1]*Fizik Bölümü, Mersin Üniversitesi, TR-33343 Mersin, Turkey*
[2]*Dept. für Physik, Universität München, Am Coulombwall 1, D-85748 Garching, Germany*
[3]*Laboratori Nazionali del Sud, INFN, Via S. Sofia 62, I-95123 Catania, Italy*
and Dipartimento di Fisica e Astronomia, Universita degli Studi di Catania, Catania, Italy
(Received 7 July 2005; published 22 December 2005)

The isoscalar giant monopole resonance (ISGMR) and isovector giant dipole resonance (IVGDR) in finite nuclei are studied within the framework of a relativistic transport approach. Small-amplitude oscillations are analyzed with the relativistic Vlasov equation, i.e., neglecting nucleon collision terms. The excitation energies of ISGMR and IVGDR are obtained for spherical nuclei with various sets of Lagrangian parameters. In the case of ^{208}Pb we study in detail the dependence of the monopole response on the effective mass and symmetry energy at saturation a_4 given by the used covariant effective interaction. We show that a reduced m^* and a larger a_4 can compensate for the effect on the ISGMR energy centroid of a much larger compressibility modulus K_{nm}. The role of the symmetry energy is confirmed by the observation of reduced corrections for the more symmetric ^{90}Zr. This result is important for overcoming the conflicting determination of nuclear compressibility between nonrelativistic and relativistic effective interactions. For symmetry-energy dynamical effects, we analyze the influence of the inclusion of an effective isovector-scalar channel, δ-meson field, with constant- and density-dependent couplings. We show that the δ-meson contribution, keeping fixed the equilibrium a_4 value, leads to a reduction in the centroid energy of the ISGMR and IVGDR for ^{208}Pb. The same mechanism can account for the apparent paradox of a decrease of the frequency of a IVGDR mode in heavy nuclei (of volume type) even in presence of a larger a_4. All that in fact reveals the sensitivity of the ISGMR and IVGDR collective motions for neutron-rich systems on the *slope* (or pressure) of the symmetry energy at saturation. Density-dependent vertices do not much affect our conclusions. Following as a guidance the dispersion relations in nuclear matter, we see two main reasons for that: The smoothness of the density dependences around saturation and the presence of compensation effects coming from rearrangement terms.

DOI: 10.1103/PhysRevC.72.064317 PACS number(s): 21.30.Fe, 21.65.+f, 24.30.Cz, 21.10.Re

I. INTRODUCTION

In this work we study the isoscalar giant monopole and isovector giant dipole oscillations in ^{208}Pb and ^{90}Zr, isoscalar giant monopole resonance (ISGMR) only, by using the relativistic Vlasov (RV) transport approach in a relativistic mean-field (RMF) theory with constant- and density-dependent meson-nucleon vertices. We analyze various RMF models with different coupling parameters that lead to a different nucleon effective mass (m^*), compressibility modulus (K_{nm}), symmetry energy (a_4), and its slope (symmetry pressure), keeping fixed other nuclear matter saturation properties. The aim of this paper is not to find the best agreement with the existing data but to clarify how the various covariant contributions to the interaction affect the collective response. The discussion is also supported by analytical results obtained in a relativistic linear response theory.

Among the various models we focus on the ones in which the scalar-isovector channel has been introduced by the coupling to an effective δ-meson field [1]. It has been shown that such an inclusion has important effects on the equation of state (EOS) and phase diagram of asymmetric nuclear matter (ANM) [1], as well as on the reaction dynamics with exotic nuclei; see the review of Ref. [2]. In fact the δ meson contributes to the slope and curvature of the symmetry energy and to the neutron-proton effective-mass splitting. In particular the influence of this coupling on the collective response of ANM appears important, as shown in a linear response approach in Ref. [3]. For the comparison of the results we also consider the well-known NL3 [4,5] parametrization, very successful for finite nuclei structure calculations, and some density-dependent vertex models [6,7] (beyond the RMF). In this way we aim to pin down the sensitivity of isoscalar and isovector collective oscillations on m^*, K_{nm}, and a_4, focusing on the interplay between isoscalar and isovector couplings. In particular we see that the covariant structure of the isovector part of the effective interaction will clearly show up even in the isoscalar-monopole mode in ^{208}Pb.

RMF models, with constant-dependent [8,9] and density-dependent [10,11] meson-nucleon couplings, are applied to the description of collective excitations of atomic nuclei within the framework of the time-dependent relativistic mean field (TDRMF) and in the self-consistent relativistic random-phase approximation (RRPA). The monopole predictions of nonrelativistic Hartree-Fock plus random-phase approximation (RPA) calculations, when both Skyrme and Gogny effective interactions are used, seem to indicate that the value of K_{nm} should be in the range 210–220 MeV [12,13]. In RMF models, on the other hand, results of both time-dependent and RPA calculations suggest that empirical giant monopole resonance (GMR) energies are best

*Electronic address: ditoro@lns.infn.it

 ©2005 The American Physical Society

reproduced by an effective force with K_{nm} 250–270 MeV [14,15]. This difference has been pointed out as a serious open problem [11]. A possible solution to this ambiguity was suggested in Ref. [3] as an interplay between the effective mass and compressibility within a discussion of the isoscalar response in nuclear matter. Here we show the validity of this interpretation, joining to a density dependence of the symmetry energy, also for the spherical finite n-rich nuclei, like ^{208}Pb. Recent studies in fact point to the same isospin effect; see Refs. [16–20]. In this respect we extend our analysis by studying the influence of the inclusion of the δ meson on both isoscalar and isovector responses in spherical n-rich nuclei.

For the isovector dipole response we also show the importance of the density dependence of the symmetry energy around saturation, in particular of its slope (symmetry pressure). Thus we can establish a clear link between the collective modes of neutron-rich nuclei and the neutron distribution on the surface of nuclei or nuclear stars.

The introduction of density-dependent vertices, following the Dirac-Brueckner- Hartree-Fock (DBHF) estimations, does not show relevant new effects. An analytical interpretation of this result, again from a linear response theory for nuclear matter, is finally presented.

II. OUTLINE OF THE MODEL

The dynamics of collective vibrations in spherical nuclei is studied within the framework of the RV transport equation, which describes the dynamical evolution of a semiclassical phase-space distribution function $f(x, p)$ under the influence of the nuclear mean field. Binary collisions between nucleons are not considered here. Thorough derivations of the RV transport equations from an effective hadron-meson field theory [21] can be found elsewhere [22–24]. The RV equation reads ($i = p, n$)

$$\left[p_i^{*\mu}\partial_\mu + \left(p_{\nu i}^{*}\mathcal{F}_i^{\mu\nu} + m_i^{*}\partial^\mu m_i^{*}\right)\partial_\mu^{(p_*)}\right] f_i(x, p^*) = 0, \tag{1}$$

with the field tensor

$$\mathcal{F}_i^{\mu\nu} \equiv \partial^\mu \Sigma_i^\nu - \partial^\nu \Sigma_i^\mu, \tag{2}$$

and effective masses and kinetic momenta m^* and $p^{*\mu}$, respectively, specified below. The particles obey the mass-shell condition

$$p_i^{*\mu} p_{i\mu}^{*} - m_i^{*2} = 0. \tag{3}$$

Thus, from the temporal knowledge of the phase-space distribution function, one can calculate the time evolution of physical quantities such as densities and fields. We remind the reader of the meaning of the the Wigner matrix (in the spinor space):

$$\begin{aligned} F_{\alpha\beta}(x, p) &= \langle \hat{F}_{\alpha\beta}(x, p)\rangle \\ &\equiv \frac{1}{(2\pi)^4}\int d^4R\, e^{-ip_\mu R^\mu} \\ &\quad\times \left\langle \bar{\psi}_\beta\left(x + \frac{1}{2}R\right)\psi_\alpha\left(x - \frac{1}{2}R\right)\right\rangle. \end{aligned} \tag{4}$$

From the above definition it follows that the mean value of single-particle operators can be expressed as (spinor indices are omitted for simplicity)

$$\langle \hat{O}\rangle = \int d^4x \int d^4p\, \mathrm{tr}[\hat{O}F(x, p)] \tag{5}$$

where the trace runs over spin and isospin indices. The scalar density and the vector current, for example, assume the forms

$$\rho_s(x) = \langle \bar{\psi}\psi\rangle = \int d^4p\, \mathrm{tr}[F(x, p)] \tag{6}$$

$$j_\mu(x) = \langle \bar{\psi}\gamma_\mu\psi\rangle = \int d^4p\, \mathrm{tr}[\gamma_\mu F(x, p)], \tag{7}$$

and are used to calculate the different Lorentz components of the mean-field potential. The nuclear mean field U is characterized in a RMF theory by means of self-energies as $U = \Sigma_s - \gamma_\mu\Sigma^\mu \cdots$ (higher contributions are usualy neglected because of the symmetry properties of nuclear matter).

The starting point of our calculation is a non-linear Quantum-Hadro-Dynamics (QHD-NL) model with isoscalar-scalar and vector-meson fields σ and ω and with the inclusion of the isovector channel through the exchange of the virtual charged δ (scalar) and ρ (vector) mesons. The interacting Lagrangian density has the form

$$\begin{aligned} \mathcal{L}_{\mathrm{int}} &= \bar{\psi}[g_\sigma\sigma + g_\delta\vec{\tau}\cdot\vec{\delta} - g_\omega\gamma_\mu\omega^\mu - g_\rho\gamma^\mu\vec{\tau}\cdot\vec{b}_\mu]\psi \\ &\quad - \tfrac{1}{3}a\sigma^3 - \tfrac{1}{4}b\sigma^4. \end{aligned} \tag{8}$$

Minimal self-interacting terms are included in only the σ channel, in order to cure the large value of the compression modulus of the original Walecka linear model [21].

The mean-field approximation leads to self-energies that are related to the expectation values of the combination of isoscalar and isovector fields with coupling constants g_σ, g_ω, g_ρ, and g_δ. The scalar and vector components of the self-energies are generally given by

$$\Sigma_i^\mu = g_\omega\omega^\mu(x) \pm g_\rho b^\mu(x) \qquad \begin{cases} +\ \text{proton}(i = p) \\ -\ \text{neutron}\ (i = n), \end{cases} \tag{9}$$

$$\Sigma_{si} = g_\sigma\sigma(x) \pm g_\delta\delta(x) \qquad \begin{cases} +\ \text{proton}\ (i = p) \\ -\ \text{neutron}\ (i = n), \end{cases} \tag{10}$$

with the expectation values of the fields self-consistently calculated; see later Eqs. (20).

The self-energies characterize the in-medium properties of the nucleons inside the hadronic environment in terms of kinetic momenta and effective masses:

$$p_i^{*\mu} = p_i^\mu - \Sigma_i^\mu, \tag{11}$$

$$m_i^* = m - \Sigma_{si}. \tag{12}$$

The density dependence of the mean field, i.e., the density behavior of the self-energies, depends on the coupling choices of the RMF model. Here we consider different parametrizations within the nonlinear (QHD-NL) effective-field approach and even extend it to the density-dependent hadronic (DDH) mean-field theory [6,7,25]. In Table I the values for the different coupling constants and the nonlinear parameters for different sets of nonlinear Walecka (QHD-NL) models are presented; for details see Refs. [1–5,7]. Their corresponding

TABLE I. Coupling parameters in terms of $f_i \equiv (g_i/m_i)^2$ for $i = \sigma, \omega, \rho, \delta$, $A \equiv a/g_\sigma^3$, and $B \equiv b/g_\sigma^4$, Eq. (8), for various nonlinear RMF models with the ρ and both ρ and δ mesons used for the characterization of the isovector mean field. In the DDH models the coupling functions are explicitly density dependent [6,7,25].

Parameter	NL1-G	NL2-G	NL3	NLρ	NL$\rho\delta$
f_σ (fm^2)	6.146	9.300	15.739	10.330	10.330
f_ω (fm^2)	3.611	3.611	10.530	5.420	5.420
f_ρ (fm^2)	1.200	1.220	1.339	0.950	3.150
f_δ (fm^2)	0.0	0.0	0.0	0.0	2.500
A (fm^{-1})	−0.123	0.0824	−0.01	0.033	0.033
B	0.169	−0.0012	−0.003	−0.0048	−0.0048

nuclear matter saturation properties are given in Table II. In the DDH models the density dependence of the coupling constants is chosen in order to reproduce microscopic DBHF results beyond the RMF picture; see the discussion in Ref. [25].

The choice of models with rather different nuclear matter properties has been made on purpose, in order to investigate the role of the effective masses, compressibility, and symmetry energy on isoscalar (monopole) and isovector (dipole) oscillations in neutron-rich nuclei. We compared various nonlinear RMF parametrizations, in particular the Giessen sets NL1-G and NL2-G, [26], which we extended also to simulations of relativistic heavy-ion collisions and the widely used NL3 set [4,5], successfully applied in finite nuclei studies. The different treatment of the isovector part of the mean field (competition effects of the repulsive ρ field and the attractive δ meson) is analyzed with the (NLρ, NL$\rho\delta$) parameter sets [1]. The same analysis is performed within density-dependent coupling models; the parametrizations DDH3ρ and DDH3$\rho\delta$ of Ref. [25] are used.

The dynamics of collective vibrations in spherical nuclei is simulated in the framework of the RV Eq. (1). Its numerical realization is based on the standard test-particle method, in which the phase-space distribution function $f(x, p)$ is represented by a finite number of test particles of a covariant Gaussian form [relativistic Landau-Vlasov (RLV) method]. A detailed description of the RLV method is given in Ref. [27]; this model is briefly discussed here. The use of a Gaussian shape for the test particles has the advantage of smooth distribution functions, but maintaining an accurate determination of local quantities, which is particularly important near the nuclear surface.

TABLE II. Nuclear matter saturation properties in the different RMF models.

Property	NL1-G	NL2-G	NL3	NLρ, $\rho\delta$	DDHρ, $\rho\delta$
E/A (MeV)	−16.0	−16.0	−16.3	−16.0	−16.0
ρ_0 (fm^{-3})	0.145	0.145	0.148	0.160	0.153
m^*/m	0.83	0.83	0.60	0.75	0.55
K_{nm} (MeV)	380	210	272	240	240
a_4 (MeV)	30.62	30.62	37.40	30.50	33.40

The covariant Gaussians in the four-dimensional Minkowski space are defined as

$$\begin{aligned} G(x;\xi_i) &\equiv \int_{-\infty}^{-\infty} d\tau\, g[x - x_i(\tau)] \\ &= \alpha \int_{-\infty}^{-\infty} d\tau\, \exp\{[x - x_i(\tau)]^2/w^2\} \\ &\quad \times \delta\{[x_\mu - x_{i\mu}(\tau)]u_i^\mu(\tau)\}, \end{aligned} \tag{13}$$

where ξ_i denotes the world line of the particle i as a whole, τ refers to the eigentime of the test particle, and α is the normalization constant. In the four-dimensional momentum space a Gaussian weight of a test particle is defined by [27]

$$\begin{aligned} g[p^* - p_i^*(\tau)] &\equiv \alpha_p \exp\{[p^* - p_i^*(\tau)]^2/w_p^2\} \\ &\quad \times \delta[p_\mu^* p_i^{*\mu}(\tau) - m_i^{*2}], \end{aligned} \tag{14}$$

where the center of the Gaussian is assumed to be on-shell, i.e., $p_{i\mu}^* = m_i^* u_{i\mu}$, $u_i^2 = 1$, whereas the free momentum p_μ^* is generally off-shell. The effective mass of the particle is taken as $m_i^* = m^*[x_i(\tau)]$. The norm of the Gaussian is calculated in the rest frame of the particle to be m_i^{*-1} with $\alpha_p = (\sqrt{\pi} w_p)^{-3}$, where w and w_p are the test-particle widths in position and momentum space, respectively.

With the Gaussians of Eqs. (13) and (14) the phase-space distribution function $f(x, p^*)$ is expressed as

$$\begin{aligned} f(x,p^*) &= \frac{1}{N}\sum_{i=1}^{AN}\int_{-\infty}^{+\infty} d\tau\, g[x - x_i(\tau)]g[p^* - p_i^*(\tau)] \\ &= \frac{1}{N(\pi w w_p)^3}\sum_{i=1}^{AN}\int_{-\infty}^{-\infty} d\tau\, \exp\{[x - x_i(\tau)]^2/w^2\} \\ &\quad \times \exp\{[p^* - p_i^*(\tau)]^2/w_p^2\} \\ &\quad \times \delta\{[x_\mu - x_{i\mu}(\tau)]u_i^\mu(\tau)\}\delta[p_\mu^* p_i^{*\mu}(\tau) - m_i^{*2}], \end{aligned} \tag{15}$$

where N is the number of test particles per nucleon. Scalar densities ρ_s and baryon currents j_μ follow from the phase-space distribution:

$$\rho_s(x) = \frac{1}{N}\sum_{i=1}^{AN}\int_{-\infty}^{-\infty} d\tau \frac{m^*(x)}{m^*[x_i(\tau)]} g[x - x_i(\tau)], \tag{16}$$

$$j_\mu(x) = \frac{1}{N}\sum_{i=1}^{AN}\int_{-\infty}^{-\infty} d\tau\, g[x - x_i(\tau)]u_{i\mu}(\tau). \tag{17}$$

The equations of motion for test particle trajectories are given by

$$\frac{d}{d\tau}x_i^\mu(\tau) = u_i^\mu(\tau), \tag{18}$$

$$\begin{aligned} \frac{d}{d\tau}u_i^\mu(\tau) &= \frac{1}{m^*(x_i)}\sum_{j=1}^{AN}\frac{2}{w^2}\left\{\frac{g_\omega^2}{m_\omega^2}u_{i\nu}\left[R_j^\mu(x_i)u_j^\nu - R_j^\nu(x_i)u_j^\mu\right]\right. \\ &\quad \left. - g_\sigma\frac{\partial\sigma(x_i)}{\partial\rho_s}\left[R_j^\mu(x_i) - u_i^\mu u_i^\nu R_{j\nu}(x_i)\right]\right\} \\ &\quad \times \frac{\exp\left[R_j^2(x_i)/w^2\right]}{N(\sqrt{\pi}w)^3} \pm \frac{1}{m^*(x_i)}\frac{2}{w^2} \end{aligned}$$

$$\times \sum_{j=1}^{ZN} \left\{ \frac{g_\rho^2}{4m_\rho^2} u_{i\nu} \left[R_j^\mu(x_i) u_j^\nu - R_j^\nu(x_i) u_j^\mu \right] - \frac{g_\delta^2}{4m_\delta^2} u_{i\nu} \left[R_j^\mu(x_i) - u_i^\mu u_i^\nu R_{j\nu}(x_i) \right] \right\} \times \frac{\exp\left[R_j^2(x_i)/w^2 \right]}{N(\sqrt{\pi} w)^3} \mp \frac{1}{m^*(x_i)} \frac{2}{w^2} \times \sum_{j=ZN+1}^{AN} \left\{ \frac{g_\rho^2}{4m_\rho^2} u_{i\nu} \left[R_j^\mu(x_i) u_j^\nu - R_j^\nu(x_i) u_j^\mu \right] - \frac{g_\delta^2}{4m_\delta^2} u_{i\nu} \left[R_j^\mu(x_i) - u_i^\mu u_i^\nu R_{j\nu}(x_i) \right] \right\} \times \frac{\exp\left[R_j^2(x_i)/w^2 \right]}{N(\sqrt{\pi} w)^3}, \tag{19}$$

with

$$R_i^\mu(x) \equiv \left[x^\mu - x_i^\mu(\tau) \right] - \left[x_\nu - x_{i\nu}(\tau) \right] u_i^\nu(\tau) u_i^\mu(\tau),$$

which is the projection of the vector $[x - x_i(\tau)]$ on the hyperplane perpendicular to $u_i(\tau)$ [27].

Here the equations for velocities, rather than for momenta, are given, within the assumption that the particle accelerations are small. In this equation particles are propagated by their respective eigentimes, and so corresponding time coordinates $x_{i0}(\tau)$ can differ. To solve the problem of different time coordinates a *system time* has been adopted for the propagation [27].

The scalar- and vector-meson fields, determined by the scalar density ρ_s and the baryonic current j_μ, respectively, result from the solution of the corresponding equations in the local density approximation (LDA):

$$\begin{aligned} m_\sigma^2 \sigma(x) + B\sigma^2(x) + C\sigma^3(x) &= g_\sigma \rho_s(x) \\ &\equiv g_\sigma \int d^4p^* \frac{m^*(x)}{E^*(x)} f(x, p^*), \\ \omega_\mu(x) &= \frac{g_\omega}{m_\omega^2} j_\mu(x) \\ &\equiv \frac{g_\omega}{m_\omega^2} \int d^4p^* p_\mu^* f(x, p^*), \\ b_\mu(x) &= \frac{g_\rho}{4m_\rho^2} j_{3\mu}(x) \\ &\equiv \frac{g_\rho}{4m_\rho^2} \int d^4p^* p_\mu^* f_3(x, p^*), \\ \delta(x) &= \frac{g_\delta}{4m_\delta^2} \rho_{s3}(x) \\ &\equiv \frac{g_\delta}{4m_\delta^2} \int d^4p^* \frac{m^*(x)}{E^*(x)} f_3(x, p^*) \end{aligned} \tag{20}$$

with $f_3 \equiv f_p - f_n$.

An important issue for the description of low-energy excitations within the RV equation is an appropriate initialization of finite nuclei before starting the phase-space evolution of the distribution function with Eq. (19). The ground state of a spherical nucleus is randomly initialized by means of the test particles with the covariant Gaussian shape in position and momentum space. After the first step of a randomly obtained initial distribution, a fit procedure in coordinate space is performed according to realistic Thomas-Fermi reference density distributions. The (n, p) scalar densities are determined by the self-consistentl solution of the equations for the effective masses $m_{p,n}^*$. With this initialization of a given spherical nucleus the temporal evolution is described by RLV equation (19). We used 100 test particles per nucleon for the transport descriptions, which yields a smooth distribution function with very good energy conservation.

For giant resonances the time dependence of collective dynamical quantities is not periodic, as giant resonances are generally not stationary states of the mean-field Hamiltonian [9]. For nonrelativistic models it has been proved that the results from the Vlasov equation are identical to results from full quantum-mechanical calculations [the time-dependent Hartree-Fock (TDHF) calculations] [28]. Because in the nonrelativistic frame the RPA is the small-amplitude limit of a TDHF calculation, one can expect that the results from the RV equation are comparable with those from RRPA calculations of the type discussed in Ref. [14]. In the small-amplitude limit the energy obtained from the frequency of the oscillation coincides with the experimental energy of the collective oscillation.

The collective dynamical variables that characterize nuclear vibrations are defined as expectation values of single-particle operators in the phase-space representation. For the isoscalar-monopole vibrations, the time-dependent monopole moment is defined as

$$\langle r^2(t) \rangle = \frac{1}{A} \int d^3x r^2 j_0(x). \tag{21}$$

In this work we applied the RLV method to isoscalar-monopole and isovector-dipole oscillations in ^{208}Pb. The excitation of an isoscalar-monopole oscillation of the initialized nucleus in its ground state is modeled by a radial expansion. This is done by the introduction of a new coordinate,

$$r_{\text{mon}} = (1 + a) r, \tag{22}$$

for each test particle. Here a is a scaling parameter, $a = 0.1$fm has been used, and the deformation of protons and neutrons is in phase.

For the isovector-dipole oscillation the following operator has been applied [29]:

$$\hat{Q}_{1\mu}^{T=1} = \frac{N}{N+Z} \sum_{p=1}^{Z} r_p Y_{1\mu} - \frac{Z}{N+Z} \sum_{n=1}^{N} r_n Y_{1\mu}. \tag{23}$$

This means an out-of-phase shift along the z axis between protons and neutrons. We used a scaling parameter of 1 fm according to Eq. (23), which causes a center-of-mass separation between protons and neutrons, while keeping unchanged the center of mass of the whole system.

III. ISOSCALAR MONOPOLE OSCILLATIONS

The study of ISGMRs in nuclei provides an important source of information on nuclear matter compressibility. The complete experimental data set on isoscalar-monopole resonances has been analyzed by Shlomo and Youngblood [30]. In fact, within a semiempirical macroscopic approach

of the systematics of GMR, it turns out that, when one is starting from finite nuclei data, the nuclear matter compression modulus K_{nm} can be fixed only within the rather wide range 200−350 MeV. A systematic theoretical work, based on nonrelativistic RPA methods with realistic effective interactions [13], was supported the lower region of the above range, around 210−220 MeV. At variance, relativistic approaches, within the same small-amplitude limits, pointed to some definitely larger values, 250−270 MeV [11]. We address the problem, studying within a relativistic framework the ISGMR in ^{208}Pb, which shows a well-established GMR at 14.1 ± 0.3 MeV [31]. Moreover, ^{208}Pb is interesting because it represents a neutron-rich nucleus, from which we can reveal even isovector effects.

As discussed in the previous section, the isoscalar-monopole oscillations are analyzed within the RV transport equation. The nuclear mean field is evaluated in the nonlinear versions of the Walecka model and in the DDH approach; see Tables I and II. We discuss the dependence of the GMR on the compression modulus, by comparing the Giessen parametrizations (NL1-G and NL2-G) with a similar value for m^* but different K_{nm}, and on the effective mass (for fixed K_{nm}), by comparing the parametrizations of Liu *et al.* with the DDH model. The latter also allows some comments on the effect of a density dependence of the couplings around the saturation point. These analyses are comparable with similar studies within the framework of a TDRMF model (see Refs. [4,14,32], and within nonrelativistic RPA calculations of the nuclear matter compressibility by use of Gogny effective interactions; see Ref. [13].

The influence of a different treatment of the isovector part of the mean field is discussed in relation to the a_4 differences of the various interactions (see Table II), more specifically focusing on the effects of the isovector, scalar δ field, i.e., by comparison of the results of parametrizations, like NLρ,NL$\rho\delta$ and DDHρ,DDH$\rho\delta$, with and without the introduction of the δ meson. We note again that the inclusion of the δ meson in the interaction leads to a stiffer symmetry energy (around saturation) and to a splitting between the (Dirac) effective masses of neutrons and protons, see the review in Ref. [2]. Also the vector component of the isovector self-energy is modified because of the enhancement of the vector, isovector ρ meson field roughly by a factor of 3.

Figure 1 shows the dynamical evolution of the monopole moment of the excited ^{208}Pb nucleus (thin curves) for those models with fixed effective mass (NL1-G, NL2-G) and different compression modulus. The ISGMR oscillation is modeled by Eq. (21). The numerical simulation of the RV equation is performed with the test-particle method of the previous section. The limited number of test particles per nucleon (100 in our case) leads to numerical fluctuations, which can be seen in Fig. 1 in terms of spurious oscillations with very low frequencies (first peaks in the Fourier energy spectra) and in terms of a partially nonperiodic evolution of

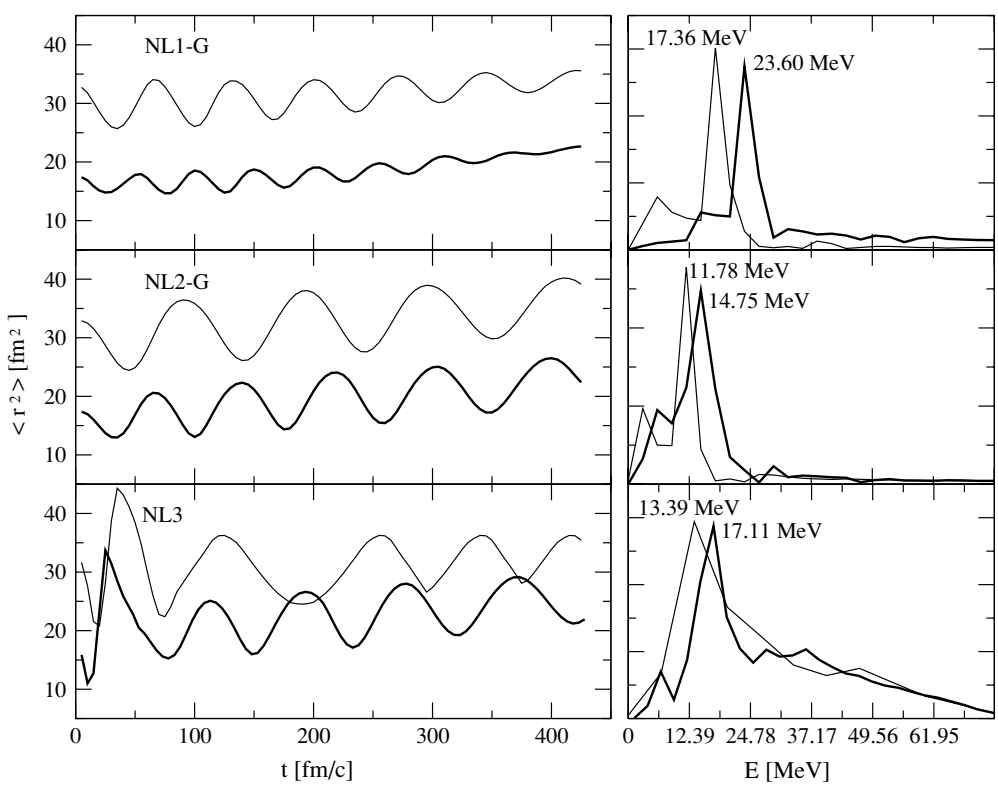

FIG. 1. (Left) Time-dependent isoscalar $\langle r^2 \rangle$ monopole moment and (right) the corresponding Fourier power spectra for ^{208}Pb (thin curves) and ^{90}Zr (thick curves), as obtained from transport calculations with different choices of the nuclear mean field: (NL1-G, NL2-G, NL3) nonlinear parametrizations of Refs. [4,26], respectively. The corresponding excitation energies of the ISGMR are indicated in the right-hand panels.

the monopole moment. This is a general nontrivial feature of transport descriptions with test-particle methods that leads to an artificial damping of the excitation [33]. However, because of a rather good stability of the nucleus (until several 100 fm/c) and a good separation of the ambiguous excitation energy of the numerical oscillations, we conclude with the reliability of the results presented in the following discussion.

The excitation energy of the ISGMR oscillation is very sensitive to the nuclear matter compressibility, which is a well-known fact. In particular, the excitation energy increases with rising compression modulus (from NL2-G to NL1-G), as expected.

The experimental value of 14.1 ± 0.3 MeV can be reproduced satisfactorily by the NL3 model [13.39 ($\hbar\omega$)]. This result is consistent with the analysis of Ref. [14], again as a good feature of the transport calculations, in spite of the completely different code, in particular for the *initialization* procedure.

We note, however, that the NL2-G model, with $K_{nm} = 210$ MeV, leads to a centroid excitation energy [11.78 ($\hbar\omega$)] that is not too far from that of the NL3 model, which has a much larger compressibility, $K_{nm} = 272$ MeV. Considering the other saturation properties of the NL3 force (see Table II), this fact is pointing to two interesting implications: (i) The dependence of the monopole frequency on the effective nucleon mass; and (ii) the dependence on the symmetry energy, value a_4, and slope around saturation that one could expect because the ^{208}Pb is a neutron-rich system, asymmetry parameter $I \equiv (N - Z)/A = 0.21$. We discuss in detail the two effects in the following subsections. We note that, as a straightforward consequence, the claimed discrepancy of the nuclear matter compressibility modulus K_{nm} between relativistic and nonrelativistic models (see [11]) can be eventually overcome.

A. Monopole frequency and effective mass

A linear response theory for nuclear matter within the RMF frame can give some interesting hints. We can derive a dispersion relation (see Refs. [2,3]):

$$1 + \frac{E_F^*}{3\,k_F^2}\left[K_{nm}^{\rm pot} - 9\,f_\omega \frac{k_F^2}{E_F^{*2}}\left(1 - f_\sigma\,\frac{m^*}{E_F^{*2}}\,\rho_S\right)\rho_B\right]\varphi(s) = 0\,, \tag{24}$$

where s is the dispersion parameter $s \equiv v_s/v_F = \omega/k \cdot v_F$ and $\varphi(s)$ is the usual Lindhard function of the Landau-Fermi liquid theory:

$$\varphi(s) = 1 - \frac{s}{2}\ln\left|\frac{s+1}{s-1}\right| + \frac{i}{2}\,\pi s\,\theta(1-s)$$

Here the $K_{nm}^{\rm pot}$ is the potential part of the nuclear matter compressibility.

From Eq. (24) we see that the "restoring" force for monopole oscillations is given by an effective compressibility that is reduced for larger values of the ω meson coupling constant. However, f_ω can assume very different values depending on the chosen value for effective masses m^*. This is easy to understand because, in the RMF limit, the saturation binding energy has the simple form

$$E/A(\rho_0) = E_F^* + f_\omega\rho_0 - m_N,$$

where m_N is the bare nucleon mass. Thus, to have the same saturation values of ρ_0, $E/A(\rho_0)$, when we decrease m^* we have to increase f_ω. We then come to the natural conclusion that two EOSs with different effective masses at saturation, even if the compressibilities are the same, are expected to have different dynamical monopole responses. In the NL2-G versus NL3 comparison discussed here we clearly see the interplay between compressibility and effective mass: We can get similar monopole energies by increasing the compressibility while decreasing the effective mass; see Table II.

This appears to be a quite general feature, present also in nonrelativistic approaches; see Fig. 7 of Ref. [13], in which the RPA systematics of the Gogny forces is shown: The ^{208}Pb breathing-mode energy does not change much if at the same time we increase the *NM* compressibility and decrease the effective mass. A similar trend has been suggested in a recent work on nuclear compressibility within the nonrelativistic frame [19].

B. Monopole frequency and symmetry energy

It is well known that the equilibrium properties of nuclear matter change with isospin asymmetry, in particular the saturation density and the corresponding EOS curvature; see [2], Sec. II and references therein. For the compressibility shift we have, after some algebra;

$$\begin{aligned}\Delta K_{nm}(I) &= 9\rho_0\left[\rho_0\frac{d^2}{d\rho^2} - 2\frac{d}{d\rho}\right]\epsilon_{\rm sym}(\rho)\Big|_{\rho=\rho_0} I^2 \\ &= [K_{\rm sym} - 6L]I^2 < 0,\end{aligned} \tag{25}$$

where $I \equiv (\rho_n - \rho_p)/\rho$, is the asymmetry parameter. We note the interplay between slope $L \equiv 3\rho_0\epsilon'_{\rm sym}(\rho)$ and curvature $K_{\rm sym} \equiv 9\rho_0\epsilon''_{\rm sym}(\rho)$ of the symmetry energy at saturation. The asymmetric matter becomes softer because the shift is in general negative, because of the dominance of the slope term L [34]; see [2] and the recent discussion in [35]. Thus, in ^{208}Pb, are n-rich system, $I = 0.21$, asymmetry can affect the isoscalar-monopole oscillations, as also noted in Refs. [16–20] within relativistic and nonrelativistic frames.

In our NL3 versus NL2-G comparison the difference in the a_4 values (see Table II), automatically implies a difference in the slope parameter L, because in both models the potential symmetry energy is coming from the effective ρ-meson coupling, which leads to a linear ρ_B dependence. Therefore the larger a_4 of NL3 means a larger slope at ρ_0 and so a larger reduction of the compressibility in ^{208}Pb; see Eq. (25). Our conclusion is that in NL3 both effects, the smaller effective mass and larger a_4, almost compensate for the much larger K_{nm} value, finally leading to a monopole frequency in ^{208}Pb that is not much different from that of the NL2-G.

We continued the analysis of the symmetry contribution, studying the effect of a scalar-isovector channel with the inclusion of the δ meson both in nonlinear and density-dependent

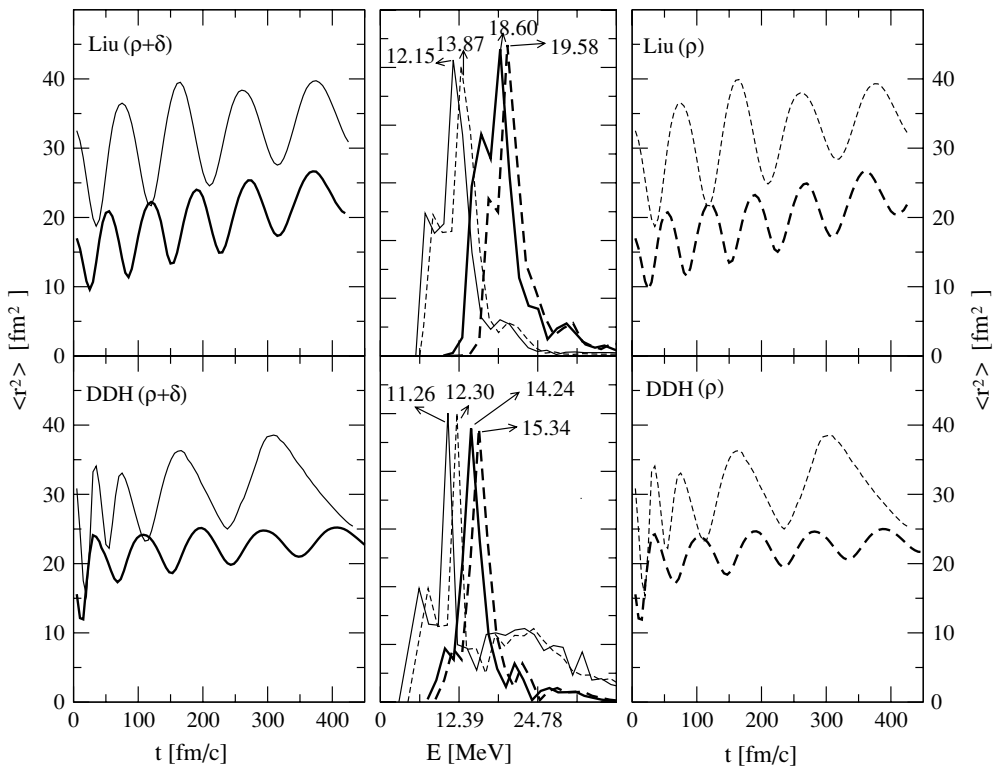

FIG. 2. (Left- and right-hand panels) Time-dependent isoscalar $\langle r^2 \rangle$ monopole moments and (middle panels) the corresponding Fourier power spectra for ^{208}Pb (thin curves) and ^{90}Zr (thick curves). Transport calculations with the parameter sets are shown: (top panels) Liu-RMF with ρ, dashed curves (right), and with $\rho + \delta$, solid curves (left). (bottom panels) Density-Dependent model (DDH) (lower panel) with ρ, dashed curve (right), and with $\rho + \delta$, solid curve (left). The excitation energy of the ISGMR for each parameter set is explicitly indicated in the Fourier power spectra and for comparison the results with $\rho + \delta$ and ρ for both parameter set 3 are shown together.

models. The results are shown in Fig. 2. The time history of the isoscalar-monopole moment and its Fourier spectrum are shown for the Liu sets in the upper panels with isovector $\rho + \delta$ interaction (NL$\rho\delta$, solid curve) and with ρ interaction (NLρ, dashed curve) and similarly with density-dependent models (lower panels). For both interactions, although the time evolution shows similar behavior, the power spectrum presents a net reduction in the energy centroid when one includes the δ meson. This is a very nice indication of the dominance of the *slope* of the symmetry energy on the compressibility shift. In fact, when the δ channel is included, we have a clear increase of the symmetry-energy slope L around saturation; see the discussion after Eqs. (6)–(19) of Ref. [2]. For example, it is about 20% larger in the Liu parametrizations.

Our discussion suggests that, although the inclusion of δ meson does not produce important effects on the ground state of finite nuclei [25], it has an interesting influence on the collective excitations of charge asymmetric finite nuclei, in particular ^{208}Pb. This appears to be a good suggestion for new experiments that aim at a better determination of the poorly known slope (and curvature) of the symmetry term around saturation.

In general the DDH monopole frequencies are systematically below the corresponding Liu ones. However this appears to be mostly a joint effect of different effective masses and symmetry energies, as already discussed for the NL3 versus NL2-G comparison. Therefore the density dependence of the coupling constants seems to not largely affect the monopole response. In fact, this can be expected from the rather smooth behavior around ρ_0; see Fig. 1 of Ref. [25]. A more detailed study is presented in Sec. V.

Finally, we like to note again that, although Liu's NLρ parametrization has a smaller K_{nm} compared with that of NL3, it produces roughly the same monopole main frequency, actually even larger. This is due to the larger effective mass jointed to the smaller a_4, see Table II. Of course we cannot compare the NL$\rho\delta$ results because the δ channel is absent in NL3.

To check the interpretation of our results as being due largely to a different density dependence of the symmetry term that can partially balance the different compressibilities, we performed the same calculations for a more symmetric system, the ^{90}Zr, $I = 0.11$, as also recently suggested [20]. The results are indicated by the thick curves in Figs. 1 and 2. From Fig. 1 we see that monopole centroid for the NL3 versus NL2-G shifts by 12% in Pb and by about 14% in the Zr case just because the balancing effect of the symmetry contribution is reduced.

The effect is even more evident when we pass from the ρ to the $\rho + \delta$ interactions in the isovector channel, Fig. 2. In the case of constant couplings (NLρ and NL$\rho\delta$, top of Fig. 2), from a shift of 13% in the Pb case (thin curves) we go to 5% for ^{90}Zr (thick curves). A similar reduction can be seen in the DDH interactions (lower panels).

IV. ISOVECTOR-DIPOLE OSCILLATIONS

In the literature only RRPA calculations have been performed so far to study the well-known isovector giant dipole resonance (IVGDR) [10]. It has been reported that, for calculations of higher multipole modes, other than monopole, the response of a nucleus is difficult to evaluate in the TDRMF [15]. The reason for this is that, because rotational invariance is broken and the differential equations have to be explicitly solved at each time step on a two-dimensional mesh in coordinate space, it becomes difficult to keep the solutions stable for the long times that are necessary for good accuracy. The problem is overcome in the present RLV simulation, as it is possible to study the time history of IVGDR within a time-dependent framework as was done in the ISGMR case.

The experimental IVGDR energy in ^{208}Pb is well known as 13.30 ± 0.10 MeV [36]. Because in the isovector channel we mainly want to study the effect of the inclusion of isovector-scalar couplings, we present results of only the models that are parametrized with and without δ mesons. In Fig. 3 we present the ^{208}Pb IVGDR oscillations and the corresponding Fourier transforms within models that include isovector-scalar channels namely Liu (upper panels) with $\rho + \delta$, solid curves (left) and ρ, dashed curves (right), and similarly for density-dependent parameter sets (lower panels). The Fourier transforms show a good single-frequency dominance of the isovector mode. We observe that the DDH models, with $a_4 = 33.4$ MeV, systematically give a larger resonance energy compared with that of Liu-RMF sets, with $a_4 = 30.5$ MeV. Moreover in both models a clear reduction of the centroid energy is observed when the δ meson is included.

It is a well-known fact that the dynamics of IVGDR is rather sensitive to the symmetry energy of the corresponding model, which is acting as a kind of restoring force parameter. The drawback in previous relativistic models is the one-to-one correspondence between a_4 and IVGDR energy [10,11], and so it is difficult to discriminate among the different interactions. This is not the case in our analysis. The new important conclusion that can be drawn from our results is that the IVGDR dynamics is also sensitive to the more microscopic covariant structure of the symmetry term, i.e., to the interplay of various isovector channels. The physical interpretation of this result can be given in terms of the isovector response derived in Ref. [3], in which it is shown that the potential part of the symmetry energy explicitly appears in the dispersion relations with an correction term having a definite f_ρ, f_δ structure:

$$1 + \frac{6\,E_F^*}{k_F^2}\left[E_{\rm sym}^{\rm pot} - \frac{f_\rho}{2}\frac{k_F^2}{E_F^{*2}}\left(1 - f_\delta\,\frac{m^*}{E_F^{*2}}\,\rho_S\right)\rho_B\right]\varphi(s) = 0 \tag{26}$$

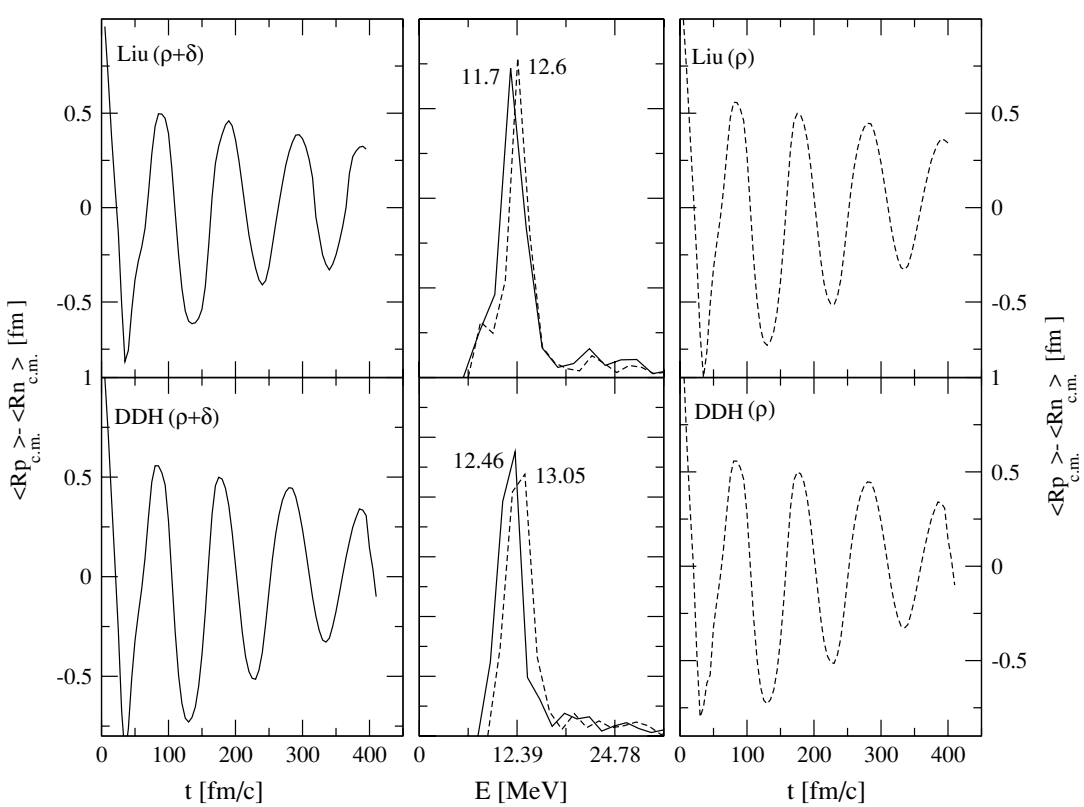

FIG. 3. Time-dependent isovector-dipole moment (center-of-mass displacement of protons and neutrons $\langle Rp_{\rm c.m.}\rangle - \langle Rn_{\rm c.m.}\rangle$) and the corresponding Fourier power spectrum for ^{208}Pb. The parameter set of the effective Lagrangian is Liu (upper panels) with ρ dashed curves (right), and $\rho + \delta$, solid curves (left), and Density Dependent model (DDH) (lower panels) with ρ dashed line (right), and $\rho + \delta$ solid curves (left). The excitation energy of the IVGDR for each parameter set is explicitly stated on the Fourier power spectrum and for comparison the results with $\rho + \delta$ and ρ for both parameter sets are shown together.

Note the similarity with the corresponding dispersion relation for isoscalar modes, Eq. (24), in particular the parallel role played by compressibility and symmetry energy in the two collective degrees of freedom.

Now we can easily have interactions with the same a_4 value at normal density but with a rather different isovector-dipole response. In fact, when including the δ channel, we have to increase the f_ρ coupling in order to have the same symmetry energy at saturation (δ, scalar field, is attractive in the isospin degree of freedom; see the discussion in Sec. VI of Ref. [2]). Then the isovector-dipole "effective restoring force" [coefficient of the Lindhard function in Eq. (26) will be reduced.

A similar effect has been pointed out in a detailed non-relativistic Skyrme-RPA study of the giant dipole resonance in heavy nuclei (^{208}Pb) bu use of effective interactions with various isovector terms [37]. A separate sensitivity of the average resonance frequencies on the symmetry energy a_4 and on its slope has been found. An intriguing consequence of this result, already noted in Ref. [37], is that in finite nuclei we can have an IVGDR energy decrease while the a_4 of the used effective force is increasing. This has been usually interpreted as an effect that is due with an increase of the symmetry slope combined with the assumption that the IVGDR is mainly a surface mode [10,20]: A stiffer behavior, which implies a larger a_4, will give a smaller symmetry energy at lower densities. This argument is not fully satisfying because the transition densities show a large-volume component, in particular for medium-heavy nuclei in which the Steinwedel-Jensen systematics appears to work quite well [38]. Our dispersion relation, Eq. (26), in fact shows that the decrease of the IVGDR centroid with increasing symmetry slope, mainly fixed by the interplay of the f_ρ, f_δ couplings, is a rather general result, valid even for "volume" modes.

In a covariant scheme we can see from Eq. (26) that such behavior can be achieved just by using two isovector fields, at the lowest order. In a sense we are suggesting a new way, through the δ-meson term, of looking at the problem of the connection between the isoscalar-isovector collective response and the effective-field structure of the interacting Lagrangian. The main objection to the introduction of a δ field is the expected increase in the symmetry repulsion at high baryon density, which is due to the decrease of the attractive δ contribution that goes with the scalar density [1,2]. In fact this is not obvious in the frame of density-dependent vertices, as suggested by DBHF calculations [25].

In any case we remind the reader that nuclear structure properties, like the collective motions discussed here, depend on the symmetry-energy behavior around normal density. Just to clarify this point we report in Table III the variation in the slopes when we pass from the ρ to $\rho + \delta$ Lagrangians used in this paper. In the table we show the corresponding values of the γ exponent of the widely used parametrization of the symmetry energy,

$$E_{\rm sym} \simeq a_4 \left(\frac{\rho}{\rho_0}\right)^\gamma,$$

around saturation density ρ_0. In correspondence the L-slope values, see Eq. (25), are indicated.

TABLE III. Symmetry energy around saturation in the different ρ, $\rho\delta$ models.

	NLρ	NL$\rho\delta$	DDHρ	DDH$\rho\delta$
γ parameter	0.90	0.99	0.80	1.05
L slope (MeV)	82.4	90.6	80.2	103.2

The effect of δ coupling is not dramatic. Moreover we see that in any case we are inside the limits ($\gamma = 0.7$–1.05) of the best estimate of the density dependence of the symmetry energy below saturation currently extracted from heavy-ion reaction studies at the Fermi energies; see the recent [35,39–41]. The L-slope values are also inside the range $L = 88 \pm 25$ MeV deduced from isospin transport studies [35,41]. Further constraints will be provided by new suggested reaction observables (see [2,42]), and new collective motion measurements, e.g., ISGMR, and IVGDR in isotopic chains.

The previous discussion more generally indicates that a dynamical observable can be more sensitive to the microscopic structure of the isovector interaction than static properties. For instance, in a careful study of the neutron distributions [43], it is clearly shown that these "equilibrium" observables are almost equally correlated to value, slope, and curvature of the symmetry term.

Finally, we see that even for the isovector dipole we cannot reveal specific contributions related to a density dependence of the coupling constants, in the sense that all the observed differences can be accounted for just in terms of symmetry energies and of isovector channels. We must say that we have not really performed an accurate analysis of this point, e.g., comparing with RMF models with exactly the same saturation properties. However, the subdominance of specific contributions of density-dependent couplings can be enlightened by analytical results, derived within a nuclear matter linear response theory, as shown in the following section.

V. NUCLEAR MATTER RESPONSE WITH DENSITY-DEPENDENT VERTICES

In previous sections, to explore the relevant physical quantities affecting the energy centroid of the collective modes, we compared results from various QHD models and parametrizations. Furthermore, for guidance on the observed effects in finite nuclei, we took advantage of the plain dispersion relations for collective modes in nuclear matter studied in Ref. [3] in the contest of QHD-NL models. However, in the DDH approach, in which meson-nucleon couplings depend on the vector (baryon) density, the relation between the coupling functions and the compressibility can be expected to be modified together with the dispersion relations for isoscalar and isovector modes.

By a comparison of results with the different parametrizations, we argued that the density dependences of meson-nucleon couplings do not carry specific contributions at least to a large extent. To corroborate such a statement, we briefly discuss the pertinent modifications of the thermodynamic quantities together with the linear response theory in nuclear

matter, showing that in DDH models most of the effect is reabsorbed by the compressibility and large corrections may be expected only for very strong density dependences of the couplings.

We remind the reader that the DDH model has all the meson-nucleon couplings dependent on the isoscalar-vector (baryon) density, defined as $\rho = \sqrt{j_\mu j^\mu}$, with j_μ defined as in Sec. II. Such a density dependence leads to rearrangement contributions that affect the vector self-energy, adding a term that at the mean field level reads as

$$\sum_\mu^R = \left(\frac{\partial f_\omega}{\partial \rho}\rho^2 - \frac{\partial f_\sigma}{\partial \rho}\rho_s^2 + \frac{\partial f_\rho}{\partial \rho} j_{3\mu} j_3^\mu - \frac{\partial f_\delta}{\partial \rho}\rho_{s3}^2\right)\frac{j_\mu}{2\rho}. \quad (27)$$

The effect of rearrangement terms on the pressure can be found in Refs. [6,7]. More relevant for our discussion is how they enter the compressibility:

$$K = 3\frac{k_F^2}{E_F^*} + 9\left(f_\omega \rho_B - f_\sigma \frac{m^*}{E^*}\frac{d\rho_s}{d\rho_B}\rho_B\right) + 9\left(\frac{df_\omega}{d\rho_B}\rho_B^2 - \frac{df_\sigma}{d\rho_B}\frac{m^*}{E^*}\rho_s\,\rho_B\right) + 9\frac{d\Sigma_0^R}{d\rho_B}\rho_B, \quad (28)$$

with

$$\frac{d\Sigma_0^R}{d\rho_B} = \left(\frac{df_\omega}{d\rho_B}\rho_B - \frac{df_\sigma}{d\rho_B}\frac{d\rho_s}{d\rho_B}\rho_s\right) + \frac{1}{2}\left(\frac{d^2 f_\omega}{d\rho_B^2}\rho_B^2 - \frac{d^2 f_\sigma}{d\rho_B^2}\rho_s^2\right). \quad (29)$$

we can see that Eq. (28) reduces to the standard formula of QHD with constant couplings when the couplings are density independent; see Ref. [2].

The linear response in nuclear matter can be derived along the same lines as in Ref. [3], but one has to redefine the vector self-energy Σ_μ, defined in Eq. (9), by adding the rearrangement term Σ_μ^R and consequently the effective kinetic momenta, defined in Eq. (11). Also once, the equilibrium Wigner matrix is consistently redefined, in the same fashion as in Ref. [3], a dispersion relation for isoscalar modes in symmetric nuclear matter can be written as

$$1 + \frac{E_F^*}{3\,k_F^2}\left[K_{nm}^{\rm pot} - 9\,f_\omega \frac{k_F^2}{E_F^{*2}} \times\left(1 - f_\sigma\,\frac{m^*}{E_F^{*2}}\,\rho_s + \frac{\rho_s^2}{E_F^*}\,\frac{df_\sigma}{d\rho_B}\right)\rho_B\right]\varphi(s) = 0 \quad (30)$$

if the terms associated with $\partial\rho_s/\partial m^*$ are discarded or, in other words, if the safe approximation $d\rho_s/d\rho_B = m^*/E^*$ is taken. We can see that most of the derivatives of the coupling functions are reabsorbed in $K_{nm}^{\rm pot}$. The difference between Eq. (24) and (30) is the last term. With some algebra, within the same approximation scheme, the contribution of density-dependent terms can be reduced to a variation of the σ coupling, from f_σ to $f_\sigma - (df_\sigma/d\rho_B)\,\rho_B$, in the correction term of Eq. (24). Because of the smoothness of the $f_\sigma(\rho_B)$ function around ρ_0, we can expect an overall variation of a few percent in the dispersion relation.

We note, however, that now the $f_\omega(\rho_0)$ is not exactly the same of QHD-NL (with scalar nonlinear terms), because the rearrangement terms also affect the relation for the binding energy, which in DDH models is given by

$$E/A(\rho_0) = E_F^* + f_\omega\rho_0 + \Sigma_0^R - m_N. \quad (31)$$

From Eq. (27) we see that Σ_0^R is given by the difference in the density slope between the scalar and the vector field. Therefore it may not be discarded in general, but is usually subdominant because of the similar density dependence of the scalar and vector coupling functions around saturation density; see Fig. 1 of Ref. [25].

The expression for the symmetry energy is not modified in DDH models which respect to QHD-NL [1] because the couplings depend on only the isoscalar-vector density. Also the dispersion relation for the isovector mode in symmetric nuclear matter is not affected by the density dependence of the couplings and the relation in Eq. (26) is still valid. However, in ANM new terms appear that are proportional to the asymmetry I and to the derivative of the ρ-like and δ-like couplings. Therefore in DDH models for exotic nuclei there is the possibility of having a modified relation between symmetry energy and dipole excitation; however, an exhaustive study of such effects goes beyond the scope of this paper.

VI. CONCLUSIONS

The aim of this work is the study of effects of the structure of the nuclear EOSs in the isoscalar and isovector sectors on collective excitations of asymmetric nuclei. Particular attention has been paid to the dynamical implications of the inclusion of a scalar-isovector contribution that is due to an effective δ-meson coupling.

We described the dynamics of the isoscalar-monopole and isovector-dipole oscillations in a relativistic transport approach based on a nucleon-meson effective-field interaction. We evaluated the time evolution of the oscillations, and then we obtained the corresponding excitation energies from the power spectra of the modes. The applications are to the n-rich nucleus ^{208}Pb, by use of a suitable choice of different effective Lagrangians.

For the monopole mode we show an interesting m^*, the effective mass, dependence of the centroid energy. This effect, joined to a symmetry-energy contribution, can account for the claimed ambiguity on the difference in compressibility moduli that produce the experimental energy of the ISGMR in ^{208}Pb between relativistic and nonrelativistic microscopic models. From the influence of the δ meson, just a systematic reduction of the peak energy, we inferred that the symmetry-energy effect on the isoscalar monopole is mainly due to variations of the slope L around saturation. This is an important result, as it could open the possibility of a direct access to this poorly known parameter from monopole data changing the neutron number in a fixed isotope. Moreover, we will be able to trace back the covariant structure of the effective interaction in the isovector channel, of relevance also for relativistic heavy-ion collisions [25].

The isovector-dipole response is directly linked to the isospin-dependent part of the nuclear EOS. The new result shown here is that the IVGDR energy is decreasing when the

δ coupling is included, keeping fixed the symmetry energy at saturation. The effect can be easily understood from the form of isovector dispersion relations in nuclear matter in a relativistic linear response approach. We can then have different IVGDR energies for effective interactions that show the same a_4 value, but with a different covariant field structure in the isovector channel. We note the similarity to the isoscalar case, just exchanging the roles of compressibility and isoscalar couplings with symmetry energy and isovector couplings.

Finally we do not see large effects from the density dependence of the effective meson couplings. This is mainly due to the smooth behavior around ρ_0. Moreover, we have shown that some compensation is also coming from dynamical contributions of the rearrangement terms.

ACKNOWLEDGMENTS

S.Y. thanks the staff of Laboratori Nazionali del Sud (LNS), INFN, in Catania for the hospitality during his visit to LNS. This work has been supported in part by Mersin University under contract no. BAB FEF FB (SY) 2004-2.

[1] B. Liu, V. Greco, V. Baran, M. Colonna, and M. Di Toro, Phys. Rev. C **65**, 045201 (2002).
[2] V. Baran, M. Colonna, V. Greco, and M. Di Toro, Phys. Rep. **410**, 335–466 (2005).
[3] V. Greco, M. Colonna, M. Di Toro, and F. Matera, Phys. Rev. C **67**, 015203 (2003).
[4] P. Ring, D. Vretenar, and B. Podobnik, Nucl. Phys **A598**, 107 (1996).
[5] G. A. Lalazissis, J. Konig, and P. Ring, Phys. Rev. C **55**, 540 (1997).
[6] C. Fuchs, H. Lenske, and H. H. Wolter, Phys. Rev. C **52**, 3043 (1995).
[7] S. Typel and H. H. Wolter, Nucl. Phys. **A656**, 331 (1999).
[8] M. V. Stoitsov, P. Ring, and M. M. Sharma, Phys. Rev. C **50**, 1445 (1994).
[9] D. Vretenar, N. Paar, P. Ring, and T. Niksic, Phys. Rev. C **65**, 021301(R) (2002).
[10] T. Niksic, D. Vretenar, and P. Ring, Phys Rev. C **66**, 064302 (2002).
[11] D. Vretenar, T. Niksic, and P. Ring, Phys. Rev. C **68**, 024310 (2003).
[12] J. P. Blaizot, Phys. Rep. **64**, 171 (1980).
[13] J. P. Blaizot, J. F. Berger, J. Decharge, and M. Girod, Nucl. Phys. **A591**, 435 (1995).
[14] D. Vretenar, G. A. Lalazissis, R. Behnsch, W. Poschl, and P. Ring, Nucl. Phys. **A621**, 853 (1997).
[15] Z. Y. Ma, N. Van Giai, A. Wandelt, D. Vretenar, and P. Ring, Nucl. Phys. **A686**, 173 (2001).
[16] J. Piekarewicz, Phys. Rev. C **66**, 034305 (2002).
[17] B. K. Agrawal, S. Shlomo, and V. Kim Au, Phys. Rev. C **68**, 031304(R) (2003).
[18] J. Piekarewicz, Phys. Rev. C **69**, 041301(R) (2004).
[19] G. Coló, N. V. Giai, J. Meyer, K. Bennaceur, and P. Bonche, Phys. Rev. C **70**, 024307 (2004).
[20] B. G. Todd-Rutel and J. Piekarewicz, Phys. Rev. Lett. **95**, 122501 (2005).
[21] B. D. Serot and J. D. Walecka, Adv. Nucl. Phys. **16**, 1 (1986).
[22] W. Botermans and R. Malfliet, Phys. Rep. **198**, 115 (1990).
[23] B. Blaettel, V. Koch, and U. Mosel, Rep. Prog. Phys. **56**, 1 (1993).
[24] P. Danielewicz, Ann. Phys. **152**, 239 (1984).
[25] T. Gaitanos, M. Di Toro, S. Typel, V. Baran, C. Fuchs, V. Greco, and H. H. Wolter, Nucl. Phys. **A732**, 24 (2004).
[26] T. Maruyama, W. Cassing, U. Mosel, S. Teis, and K. Weber, Nucl. Phys. **A573**, 653 (1994).
[27] C. Fuchs and H. H. Wolter, Nucl. Phys. **A589**, 732 (1995).
[28] H. Stoecker and W. Greiner, Phys. Rep. **137**, 277 (1986).
[29] D. Vretenar, N. Paar, P. Ring, and G. A. Lalazissis, Nucl. Phys. **A692**, 496 (2001).
[30] S. Shlomo and D. H. Youngblood, Phys. Rev. C **47**, 529 (1993).
[31] D. H. Youngblood, H. L. Clark, and Y. W. Lui, Phys. Rev. Lett. **82**, 691 (1999).
[32] B. Podobnik, D. Vretenar, and P. Ring, Z. Phys. A **354**, 375 (1996).
[33] A. Smerzi, A. Bonasera, and M. Di Toro, Phys. Rev. C **44**, 1713 (1991).
[34] In fact, the symmetry-energy curvature is negative for most effective interactions (we have also a negative contribution from the kinetic part). It can be slightly positive for only a high increase, of a parabolic type, in the potential contribution around the saturation point; Ref. [2].
[35] L. -W. Chen, C. M. Ko, and B.-A. Li, Phys. Rev. Lett. **94**, 032701 (2005).
[36] J. Ritman *et al.*, Phys. Rev. Lett. **70**, 533 (1993).
[37] P. G. Reinhard, Nucl. Phys. **A649**, 305c (1999).
[38] A. van der Woude and H. K. Harakeh, *Giant Resonances: Fundamental High-Frequency Modes of Nuclear Excitation* (Oxford University Press, New York, 2001), p. 1.
[39] D. V. Shetty, S. J. Yennello, and G. A. Souliotis, Density Dependence of the Symmetry Energy and the EOS of Isospin Asymmetric Nuclear Matter, nucl-ex/0505011(v2).
[40] Lie-Wen Chen, Che Ming Ko, and Bao-An Li, Nuclear Matter Symmetry Energy and the Neutron Skin Thickness of Heavy Nuclei, nucl-th/0509009.
[41] Lie-Wen Chen, Che Ming Ko, and Bao-An Li, Phys. Rev. Lett. **94**, 032701 (2005).
[42] R. Lionti, V. Baran, M. Colonna, and M. Di Toro, Phys. Lett. **B625**, 33 (2005).
[43] R. J. Furnstahl, Nucl. Phys. **A702**, 85 (2002).